

Seismic Evaluation of New Steel Infill Panels for Steel Shear Walls

Ali Joharchi ^{1*}, Siti Aminah Osman ¹, Mohd Yazmil Md Yatim ¹, Mohammad Ansari ¹

¹ Department of Civil Engineering, Universiti Kebangsaan Malaysia, UKM, 43600 Bangi, Selangor, Malaysia.

Received 10 January 2021; Revised 17 March 2021; Accepted 27 March 2021; Published 01 April 2021

Abstract

Corrugated Steel Shear Wall (CSSW) is an efficient shear wall system, which has higher energy dissipation capacity, ductility and stiffness when compared to the Steel Plate Shear Wall (SPSW) with flat infill plate. Despite of these advantages, the ultimate load of CSSW is lower than that of SPSW. Various studies conducted to improve the cyclic behavior of CSSW revealed that increasing corrugation angle might enhance energy dissipation capacity and toughness of CSSWs. However, the ultimate load of CSSW was not improved by increasing the corrugation angle. Thus, the current study proposed new corrugated infill panel schemes to improve the ultimate load of CSSWs. To this end, Finite Element (FE) models were established using ABAQUS/Standard and verified with the experimental results from previous researches. The corrugation angle of the proposed plates was found based on a numerical investigation on seven CSSW FE models with the corrugation angle ranges from 30° to 120°. The FE results revealed that the model with the corrugation angle of 120 achieved highest ultimate load, energy dissipation capacity and toughness amongst the CSSW models. In addition, the ultimate loads, energy dissipation capacities and toughness of the proposed infill plates were up to 11.8%, 53.9% and 8.8% respectively higher than those of CSSW model with the corrugation angle of 120°. Furthermore, the proposed infill plates use up to 13.4% lower amount of steel compared to the corrugated plate with the corrugation angle of 120.

Keywords: Steel Plate Shear Wall; Corrugated Steel Plate; Corrugation Angle; Cyclic Loading, Finite Element.

1. Introduction

Steel Plate Shear Wall (SPSW) is an economic and highly efficient lateral load resisting system suitable for steel structures in seismic hazard zones, due to its high strength, ductility, stiffness and energy absorption capacity. The steel shear wall consists of boundary frame and an infilled steel plate. The behavior of SPSWs is mostly affected by the early elastic buckling of the infilled plate. Several experimental and numerical studies revealed that welding stiffeners to the infill steel plate could improve the stiffness and strength of SPSWs [1–3]. However, welding stiffeners is a time-consuming procedure and mainly increase the cost of construction. Using corrugated steel plate is another way to improve the buckling resistance of the thin steel plate. To date, several numerical and experimental studies have investigated the behavior of Corrugated Steel Shear Walls (CSSW) with curved and trapezoidal corrugated steel plate under monotonic and cyclic loading. Based on the comparison of the numerical results [4–6], trapezoidal CSSWs depicted slightly higher ultimate load, energy dissipation and toughness compared to the curved CSSWs. Furthermore, the connection between thin steel plate and boundary frame is easier for the trapezoidal corrugated plate.

* Corresponding author: ali.joharchi1984@gmail.com

<http://dx.doi.org/10.28991/cej-2021-03091678>



© 2021 by the authors. Licensee C.E.J, Tehran, Iran. This article is an open access article distributed under the terms and conditions of the Creative Commons Attribution (CC-BY) license (<http://creativecommons.org/licenses/by/4.0/>).

In Recent decade, numerous experimental and numerical studies have established to evaluate the behavior of the trapezoidal CSSWs. Berman and Bruneau [7] studied the behavior of SPSWs under cyclic loading using three half-scale specimens including a corrugated infill plate and two flat infill plate specimens by means of an experimental research. Shon et al. [8] experimentally studied the behavior of two vertically- and horizontally- trapezoidal CSSW specimens under cyclic loading. The experimental results showed that the corrugation direction did not make much difference in the structural behavior and energy dissipation capacity of the specimens, while it affected the failure mechanism.

Emami et al. [9] performed an experimental study on the cyclic behavior of the trapezoidal CSSWs using two vertically- and horizontally- trapezoidal CSSW specimens and a SPSW specimen with flat infill plate. The obtained results showed that the initial stiffness, energy dissipation capacities and ductility ratios of the CSSW specimens were about 20%, 40% and 52% higher than the SPSW specimen. However, the ultimate strength of SPSW specimen was 17% higher compared to CSSW specimens. In other researches, the impact of corrugation angle (30° , 45° , 60° , and 90°) and infill plate thickness (1.25, 2, 3 and 4 mm) on the behavior of the horizontally- trapezoidal CSSWs have been numerically investigated [10-12]. It was concluded that increasing the corrugation angle improved more or less the energy dissipation and ductility as well as reducing the pinching effect of the hysteresis loops. However, increasing the corrugation angle did not improve the ultimate load of CSSWs unless when using thicker plate. The experimental and numerical investigation on the vertically- trapezoidal CSSWs also showed that increasing corrugation angle could not enhance the ultimate load of the vertically- trapezoidal CSSWs.

Hosseinzadeh et al. [13] experimentally investigated the performance of vertically- trapezoidal CSSW with the corrugation angle of 30° , 45° and 60° . The results reveal that increasing the corrugation angle from 30° to 60° reduced the ultimate load of the specimens. Fadhil et al. [14] performed a numerical investigation on the trapezoidal CSSW with both vertical and horizontal corrugated plate. The corrugation angle of the infill plate ranged from 10° to 90° . The numerical results indicated that despite the hysteresis loops of the models enlarged by increasing the corrugation angle from 10° to 90° , the highest ultimate load belonged to the models with the corrugation angle of 10° .

The above literatures stated that the ultimate load of CSSW is lower than that of the SPSW with flat infill plate. Increasing corrugation angle is not much efficient on the ultimate load of CSSW. Moreover, increasing corrugation angle and thickness of the infill plate requires consuming more steel material, which consequently increases the construction cost. Hence, an efficient infill panel is needed to earn higher ultimate load, energy dissipation and toughness compared to the corrugated plates.

On basis of the aforementioned problem, this study proposed new infill plate configurations based on a combination of flat and trapezoidal corrugated plate to optimize the amount of material consumption and also to achieve a reasonable ultimate load, energy dissipation capacity, toughness and stiffness. For this purpose, numerical models were developed and verified using the experimental results conducted by Emami et al. [9]. Then, parametric study was conducted on vertically- trapezoidal CSSWs to find the most favorable corrugation angle for designing the proposed infilled plate configuration. Finally, the performance of the CSSW with the proposed infilled plate design was evaluated by comparing its numerical results with the numerical results of vertically- trapezoidal CSSWs and the SPSW made of flat infill plate. Figure 1 shows the methodology of the study

2. Finite Element Modeling

2.1. Model Description

Nonlinear FE analysis was employed to study the behavior of CSSWs under cyclic loading using ABAQUS/Standard software. The specifications and material properties of all the components of the FE model used in this study were adopted from the experimental test specimen (Sample No. 1 and 2) conducted by Emami et al. [9]. The first specimen was made of a boundary frame and a flat infill steel plate, and the second specimen contained a similar boundary frame and a vertically corrugated infill steel plate as detailed in Figure 2 and Figure 3, respectively. The boundary frame included I sections of HE-B140, HE-B200 and HE-B160, which were used for the top beam, bottom beam and columns, respectively. Moreover, the frame components were reinforced by means of stiffener plates. Steel plate which trapezoidal corrugated with a corrugation depth and flat width of 50 mm and 100 mm, respectively, were used as the infill panel with dimensions of 1480×2000 mm and thickness of 1.25 mm shown in Figure 3.b.

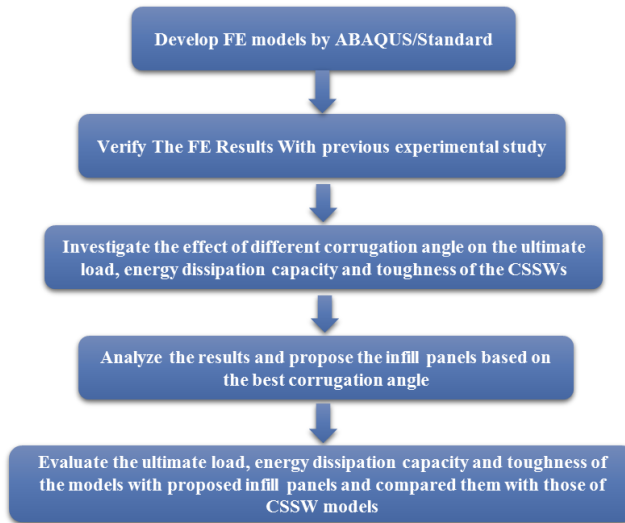


Figure 1. Methodology of the study

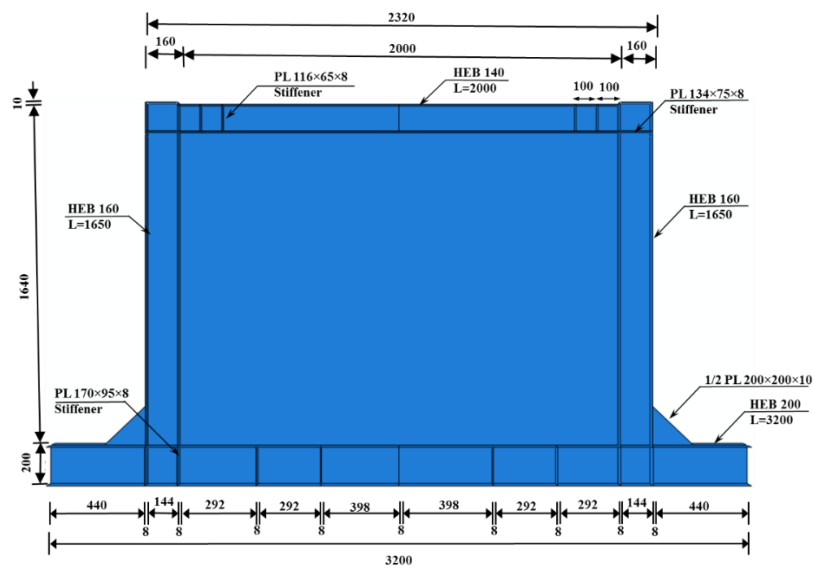


Figure 2. Detail of FE model with flat infill steel plate (unit: mm)

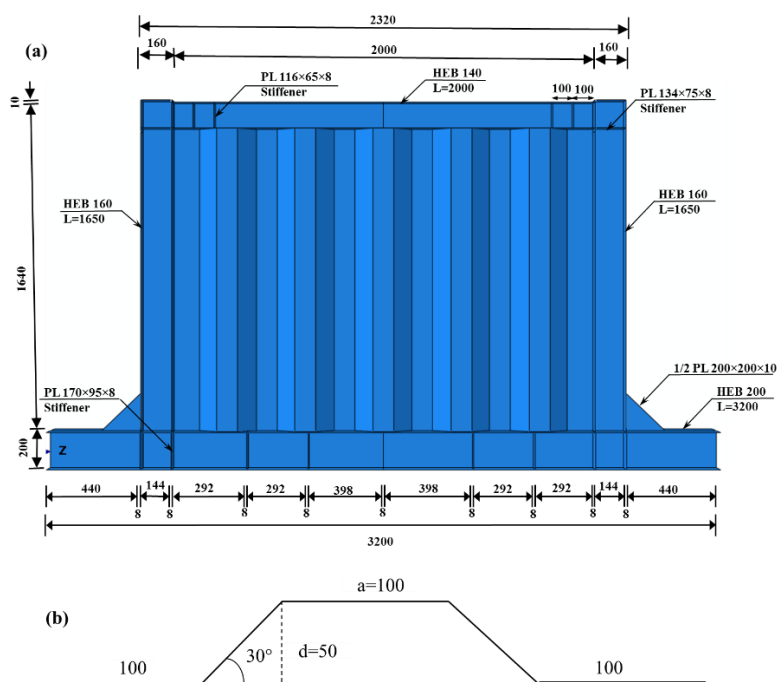


Figure 3. Detail of FE model (mm) a) the model with trapezoidally corrugated plate; b) Infill panel with a corrugation angle of 30°

2.2. Material Properties

The material properties of all components in this study were adopted from experimental test conducted by Emami et al. [9]. For the steel material in the FE model, the isotropic bilinear stress-strain relationship was assumed with similar properties for both tension and compression. The yield criteria of Von Mises was used to specify the material yield surface, as well as a related flow rule to evaluate the plastic deformation. The material properties of the components were presented in Table 1. The steel Poisson's ratio was 0.3.

Table 1. The mechanical properties of the steel components

Type	Young's Modulus E (GPa)	Yield stress f_y (MPa)	Ultimate Stress f_u (MPa)	f_y/f_u	Elongation (%)
Plate	210	207	290	0.71	41
Column	210	300	443	0.67	33
Beam	210	288	456	0.63	37

2.3. Elements Description

To model beams, columns and plates of steel shear wall, a four-node Shell element with reduced integral S4R has been used that is shown in Figure 4. This element has six degrees of freedom in global coordinates in each node and can model large strains and displacements.

The S4R element is an isotropic element, meaning the same shape functions have been used to calculate the spatial displacement field and element geometry [13]. This element uses an integration point in the middle of its surface which reduces the time of structural analysis and increases the results accuracy. In this element, by default, five integration points by thickness are used, which are sufficient to simulate the elastoplastic behavior of the shell structures.

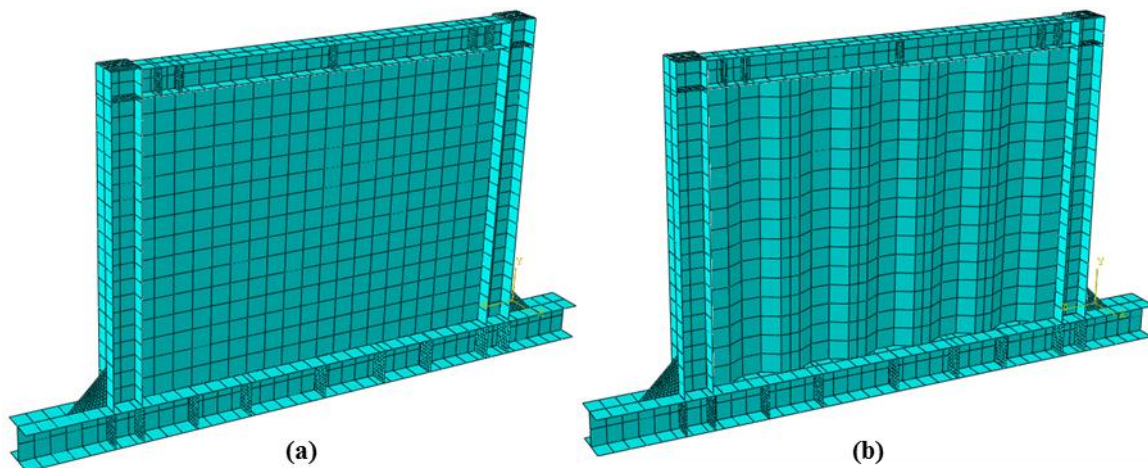


Figure 4. The S4R element in 3-D FE model (a) model with flat infill plate (b) model with corrugated infill plate

2.4. Surface Interaction

The interaction between the shear wall component surfaces is one of the most significant parameters needed for efficient modeling of the proposed FE model. In the experimental test, the frame components were connected to each other using welding. The infill plate was welded and bolted to the frame to avoid any probable failure in the connection. In fact, proper design of the connections would be very important since the steel infill panel can undergo post-yield stage if no failure occurs in the connections. Any failure in the connection between the steel plate and the frame can lead to loss of the shear wall strength. Since no failure in the connections was recorded in the experimental study [9], tie constraint was utilized for the connection between all the elements of the FE model with presumption that the connection was properly designed.

2.5. Boundary Condition and Loading Program

Fix support assigned to the base beam's bottom flange in the FE models and the translation of nodes at the top beam restricted in global X-direction, as shown in Figure 5. This scenario was conducted in the experimental test to avoid the uplift force and constrain the horizontal and out-of-plane movements. In the global Z-direction, a tabular displacement load was assigned to the exterior column flange at top of the frame, which reflected the horizontal cyclic loading. The cyclic consequence loading was adopted from the experimental test [9] as indicated in Figure 6.

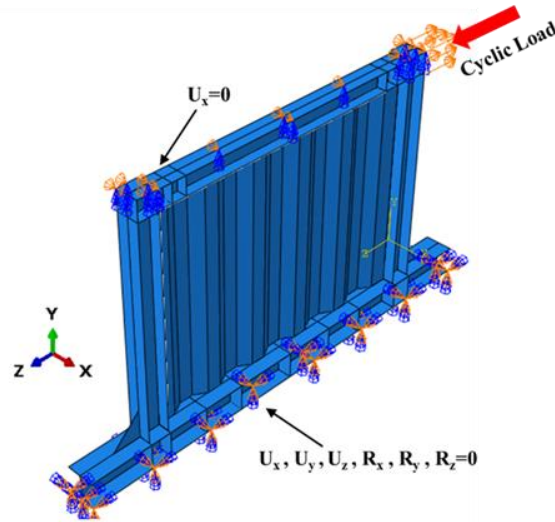


Figure 5. The boundary conditions of the FE model

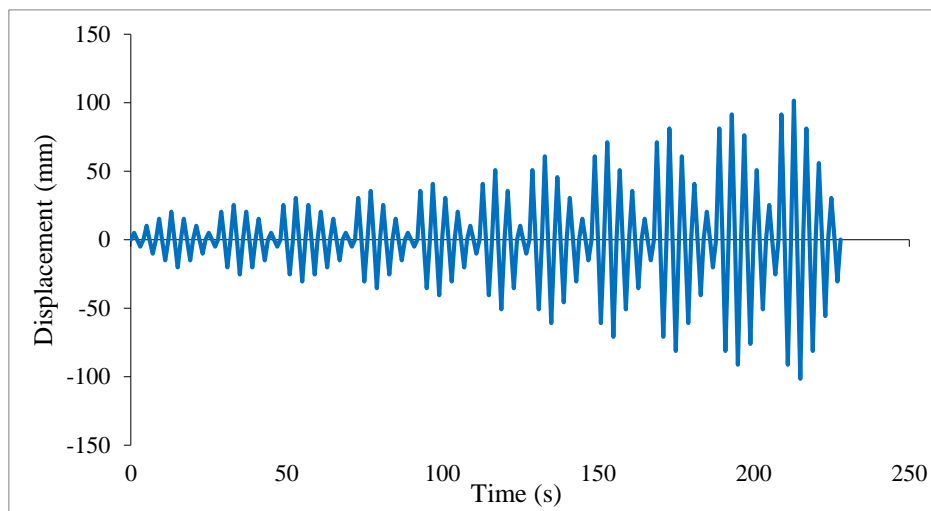
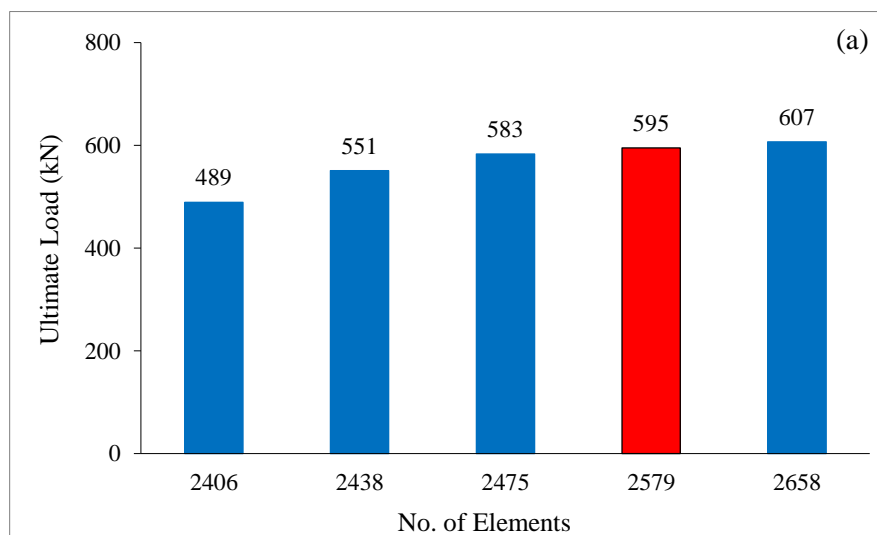


Figure 6. Cyclic displacement load consequences of the FE model

2.6. Meshing Convergence Study

A convergence research was undertaken for the numerical analysis of the FE models to achieve the correct meshing scale for the proposed FE models. The ultimate load capacities of five FE models with specific number of elements were compared to the experimental result [13]. No major difference was found between the load values of the last two iterations, as shown in Figure 7. Since the software requires a fair amount of system running time on a standard PC with higher number of elements, the models with 2475 and 3153 elements were chosen to reflect the FE models with flat and corrugated infill plate, respectively.



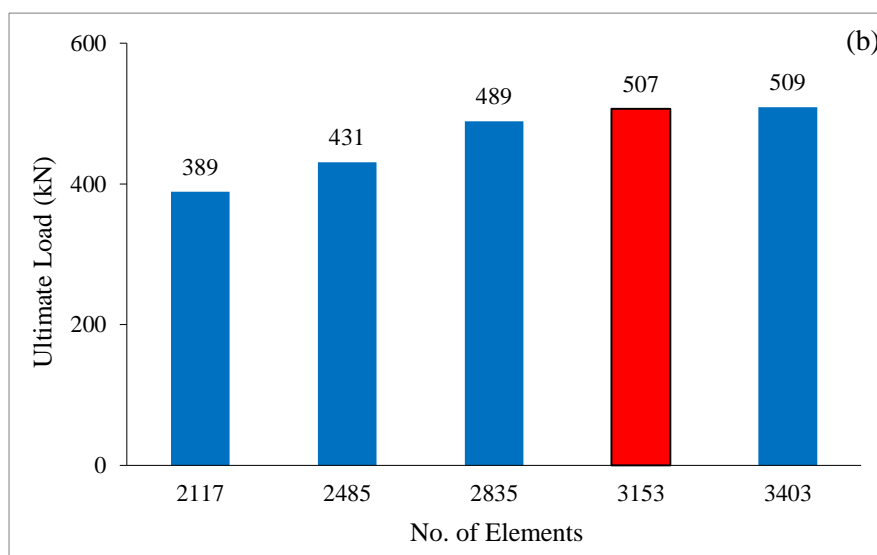


Figure 7. Meshing Convergence Study (a) model with flat infill plate (b) model with corrugated infill plate

3. Validity of FE Modelling

The accuracy of the FE models was verified by comparing the lateral load vs displacement hysteresis results and failure modes of FE analysis and their corresponding experimental results conducted by Emami et al. [13]. The models with flat infill plate and trapezoidal corrugated steel plate were referred by the specimens No. 1 and No. 2 in the experimental test, respectively. Figures 8 and 9 compare the lateral load vs displacement hysteresis results of the FE analysis and the experimental test, which show the hysteresis loops of the FE analysis were well matched with those of the experimental test. Table 2 presents a comparison between the results obtained from FE analysis and the experimental test, which indicates that the FE analysis overestimated the ultimate lateral loads of the specimens No. 1 and 2 by approximately 1% and 3%. Figure 8 displays the deformed shape of the FE model. Severe buckling of the infill plate was observed in both the experimental test and FE results. In addition, the buckling of triangular plates was also observed in both FE result and the experimental test. Figure 10 shows the deformed shapes of the FE models.

Table 2. Comparison of FE analysis and the experimental test results

Specimens	Ultimate load (kN)		FE/EX Ultimate load
	EX	FE	
No 1	580	595	1.03
No 2	500	507	1.01

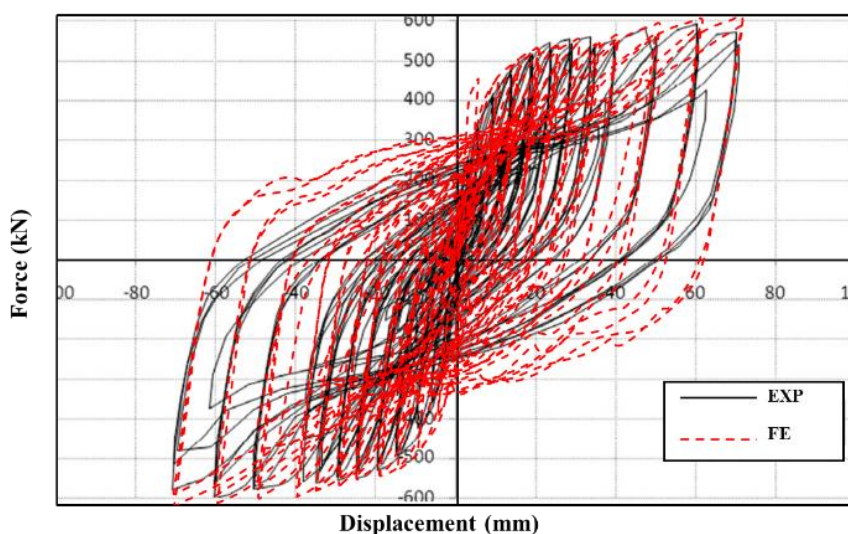


Figure 8. Comparing the lateral load vs. displacement hysteresis results (specimens No. 1)

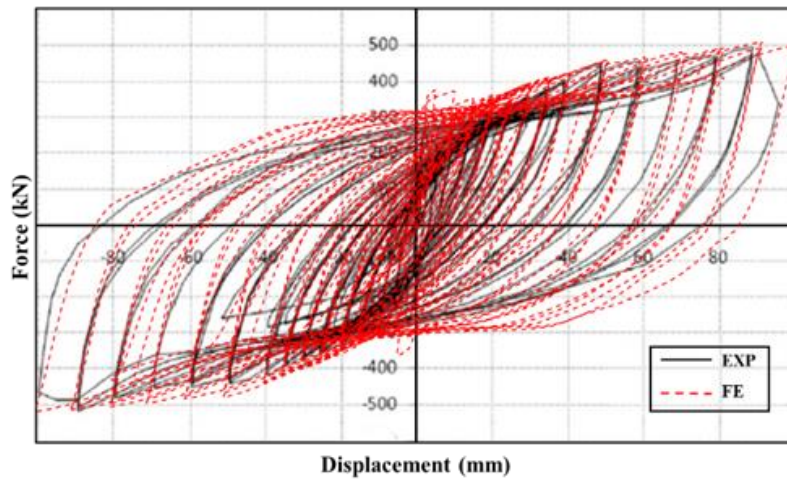


Figure 9. Comparing the lateral load vs. displacement hysteresis results (specimens No. 2)

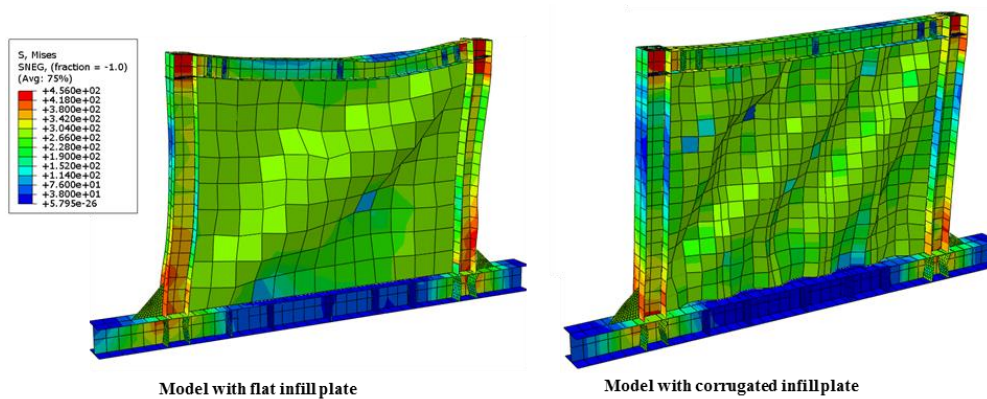
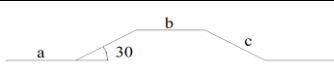
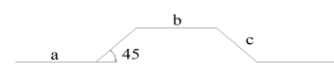
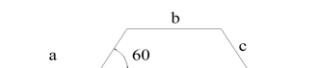
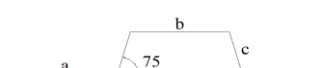
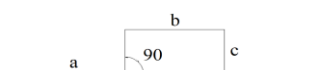
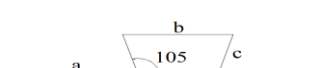
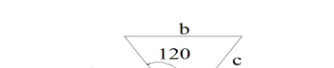


Figure 10. Von Mises stress and deformation of the FE models

4. Parametric Study

In this study, the influence of corrugation angle on the hysteretic behavior, ultimate lateral load, energy dissipation capacity, toughness of CSSWs were investigated by means of seven FE models with corrugation angles (θ) of 30°, 45°, 60°, 75°, 90°, 105° and 120°. For all models, the width of the flat parts and depth of the corrugated infill plate were 100 and 50 mm, respectively, as shown in Table 3. Furthermore, the other parameters such as the material properties, the boundary frame specifications and infill plate thickness were similar to the experimental specimens as described in Section 2.2.

Table 3. Corrugated plate sections

Model	Section	Angle	a (mm)	b (mm)	c (mm)
C30		30	100	100	100
C45		45	100	100	70.71
C60		60	100	100	57.73
C75		75	100	100	51.76
C90		90	100	100	50
C105		105	100	100	51.76
C120		120	100	100	57.73

In order to identify the model’s properties easily (the type and corrugation angle of the infill plate), the CSSW models were labeled with letter “C” and the number next to that represents the corrugation angle. While, the FE model with flat infill plate labeled with “FL”.

Figure 11 displays the hysteresis curves of the FE models. As observed in Figure 11, the pinching effect in the hysteresis loops of the models was reduced with an increase of the corrugation angle, which leads to wider and spindle-shaped loops.

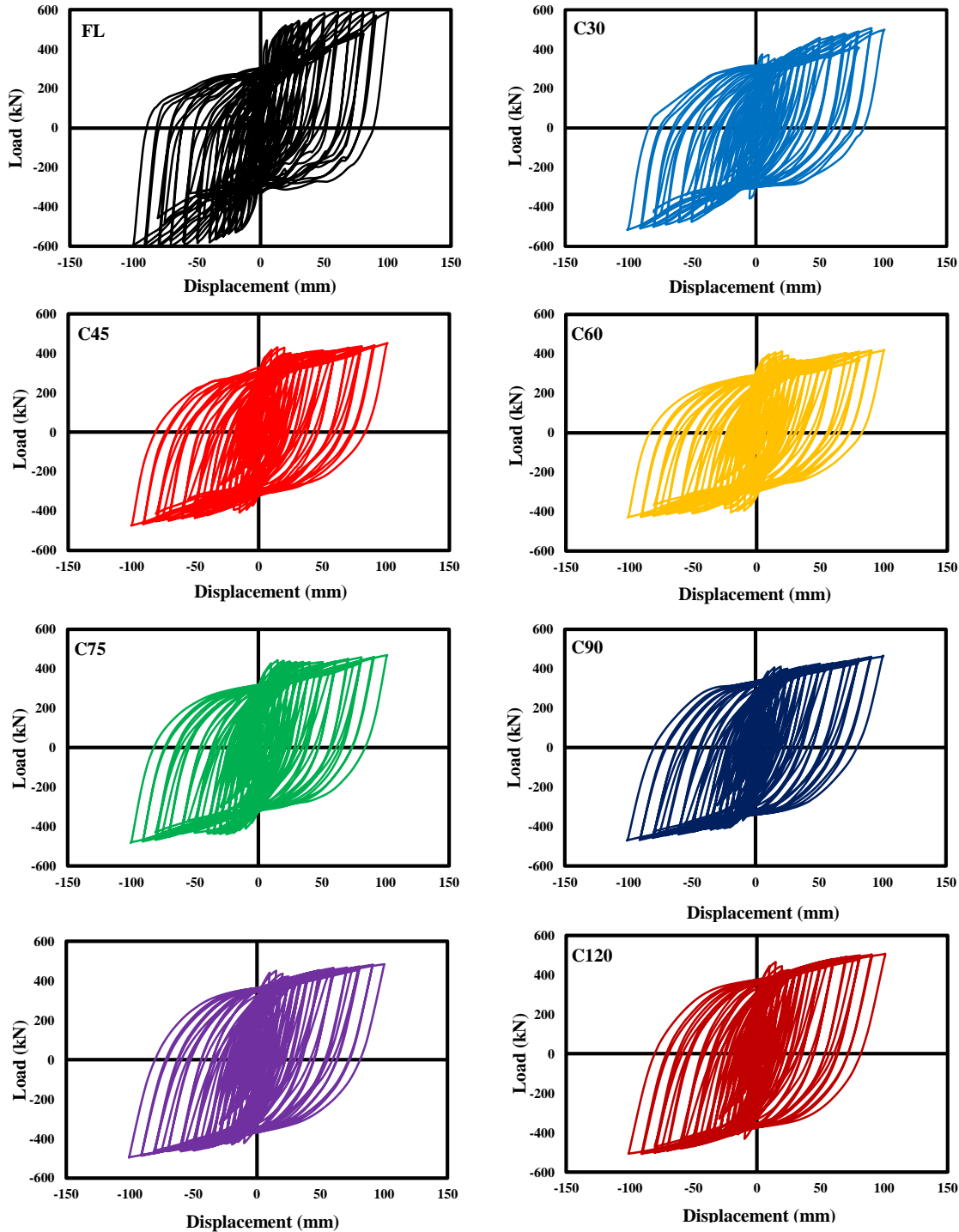


Figure 11. Hysteretic curves of the FE models with different corrugation angles

Table 4 presents the ultimate loads of the FE models. The comparison of the results show that the ultimate load of the models decreased 16.9% as the corrugation angle increased from 30° to 60°, and then improved more or less by increasing the corrugation angle from 60° to 120°. The experimental research on the vertically- trapezoidal CSSWs also showed that the CSSWs gained lower ultimate load as the corrugation angle increased from 30° to 60° [13]. In

other study on the vertically- trapezoidal CSSWs, Fadhil et al. [14] also found a reduction in the ultimate load of the FE models by increasing the corrugation angle up to 60°, and then the ultimate loads improved with an increase of corrugation angle from 60° to 90°. Furthermore, the hysteresis loops of the FE models got wider and more stable cyclic behavior as the corrugation angle increased, which is also in good agreement with the FE results of the current study. Figure 12 compares the ultimate loads of the CSSW models (Vu-C) with that of the model with flat infill plate (Vu-FI). It is observed that C30 and C120 achieved Vu-C/Vu-FI of 0.85, which is highest value amongst the other FE models.

Table 4. The results of the FE models with different corrugation angle

Model	Corrugation Angle	Ultimate Load (kN)	Energy Dissipation Capacity (kN.m)	Toughness (kN.m)
FI	0	595	756.2	36.6
C30	30	507	1002.4	43.1
C45	45	452	1038.3	41.4
C60	60	421	960.6	38.7
C75	75	469	1084.1	43.3
C90	90	466	1043.2	41.2
C105	105	483	1134.6	43.9
C120	120	505	1152.9	45.6

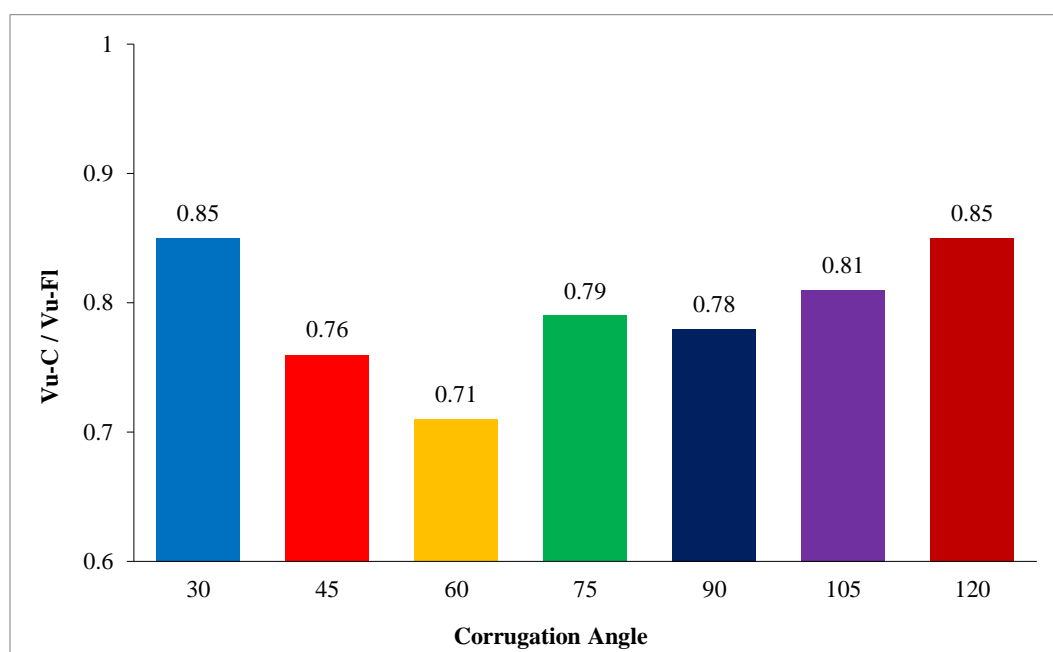


Figure 12. Comparison of the ultimate loads of the CSSW models with FI

Table 4 also presents the energy dissipation capacities of the FE models. It is observed that except in the case of 60° and 90°, increasing the corrugation angle from 30° to 120° enhanced the energy dissipation capacities of the FE models up to 15%. Figure 13 shows the ratios of the energy dissipation capacities of the CSSW models to the energy capacity of FI (DE_C / DE_{FI}). From Figure 13, C60 achieved DE_C / DE_{FI} of 1.27, which was the lowest value of DE_C / DE_{FI} among the other CSSW models. The values of DE_C / DE_{FI} revealed 52% improvement in the energy dissipation capacities of the CSSW models compared to the energy capacity of FI, when the corrugation angle of infill plate was 120°.

The toughness of the FE models is provided in Table 4. The results show that the model's toughness reduced 10.2% by increase in the corrugation angle from 30° to 60° and increased 17.8% as the corrugation angle increased from 60° to 120°. Figure 14 compares the CSSW model's toughness (T_C) with that of FI (T_{FI}). The results of T_C / T_{FI} indicated that C30 achieved T_C / T_{FI} of 1.18%. Whilst, increasing the corrugation angle from 30° to 120° increased the T_C / T_{FI} to 1.25.

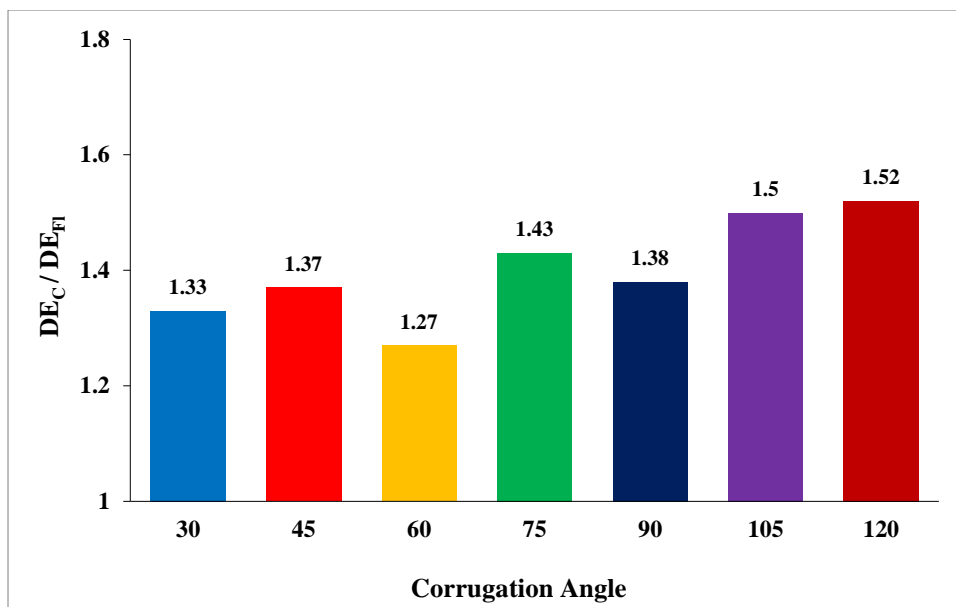


Figure 13. The ratios of the energy dissipation capacities of the CSSW models to the energy capacity of the model with flat infill plate

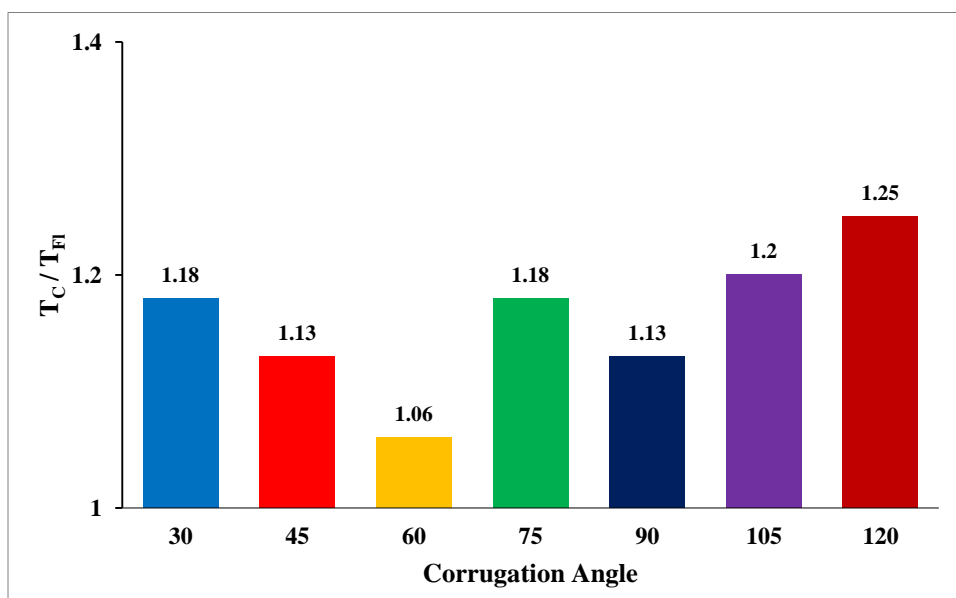


Figure 14. Comparison of the CSSW models' toughness with the flat infill plate

Based on the comparison of the results, C120 achieved the highest ultimate load, energy dissipation energy capacity and toughness amongst the FE models with corrugated infill plates. Moreover, although the ultimate load of C120 was 15% lower than that of FI, the energy dissipation capacity and toughness of C120 were 52% and 25% higher compared to those of FI, respectively. It is noteworthy that the authors numerically investigated the effect of thickness and the height-to-width ratio of the infill plate in an unpublished research. The results showed that the models with the corrugation angle of 120° gained the highest ultimate load, energy dissipation capacity and toughness compared to the corresponding models, regardless the thickness and the height-to-width ratio of the infill plate. The ultimate shear force carried by the steel shear walls is determined through two mechanisms, pure shear and diagonal tension field as presented in Equation 1 [9].

$$V_w = Lt(\tau_{cr} + 1/2\sigma_{ty}\sin2\alpha) \tag{1}$$

Where; τ_{cr} , σ_{ty} , α , L and t are the critical shear buckling stress, tension field stress, tension field angle, total length of flat sub panel, and thickness of the infill plate, respectively.

The pure shear in SPSWs with a thick infill plate generates steady plastic cyclic behavior due to widespread shear yielding. Therefore, pinching effects would be reduced in the hysteresis loops [3]. The pure shear mechanism could be improved by increasing corrugation angle due to increase in critical buckling shear stress. It could also cause a

reduction in the tension field mechanism due to increase of the tension field inclination angle, as shown in Figure 15. Therefore, the ultimate load of the models reduced as the corrugation angle increased from 30 to 60 due to the reduction in the tension field mechanism. Meanwhile, the total length of flat subpanels (L) considerably enlarged by increasing the corrugation angle from 60° to 120° , which leads to higher ultimate load.

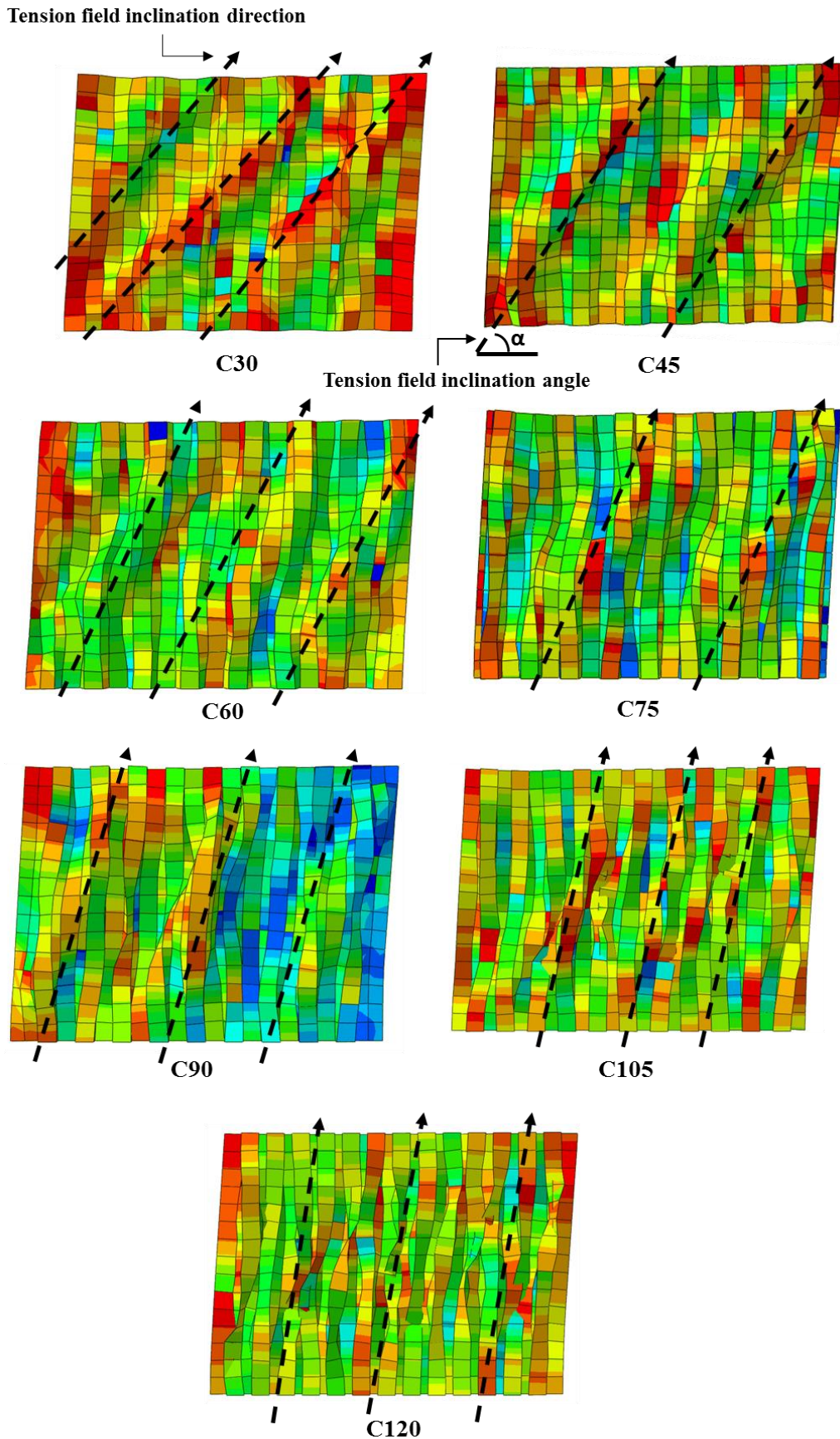


Figure 15. The tension field inclination angles of the CSSW models

5. Proposed Infill Plate

This study proposed two infill plate configurations to increase the ultimate load of CSSWs as well as optimizing the amount of steel consumption used for the infill plate. The proposed infill panels were a combination of flat and trapezoidal corrugated plates. Figure 16 shows the models with the proposed infill panels, which were labeled with “CS120” and “CM120”, respectively. Berman et al. [15] and Lv et al. [16] reported that the tension field in the infill plate occurs in three zones. Zone one and three were at the side of plate and zone two was at the middle of plate. Each zone has its own tension field inclination angle as shown in Figure 17. In this research, same concepts were utilized to design the proposed infill panels. For CS120, the flat part with the width of one-third of the total infill panel was located at the middle of the panel, while the rest of the panel was corrugated. On the contrary, in case of CM120, one-third of total infill panel width at the middle of the infill panel was corrugated and the rest of the panel kept flat while the flat part with the width of one-third of the total infill panel located at the middle of the panel, while the rest of the panel was corrugated. For CS120, the flat part with the width of one-third of the total infill panel located at the middle of the panel, while the rest of the panel was corrugated. On the contrary, in case of CM120, one-third of total infill panel width at the middle of the infill panel was corrugated and the rest of the panel kept flat. The corrugation angle, depth and flat part of the corrugation were 120°, 50 mm and 100 mm respectively for both models. Furthermore, the other parameters of CS120 and CM120 such as the specification of boundary frame, infill plate thickness and material properties were similar to the experimental test as described in Section 2.1.

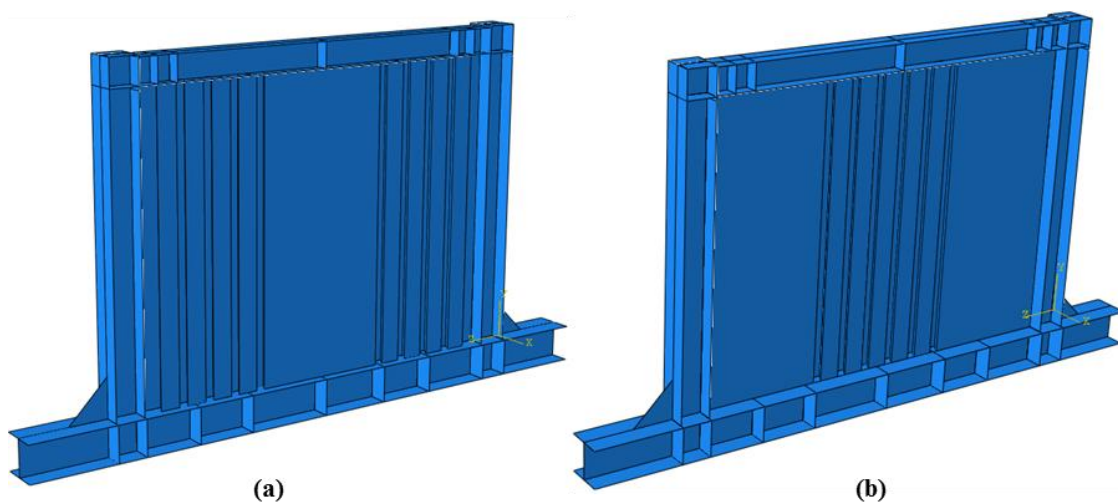


Figure 16. Configurations of the models with proposed infill plates (a) CS120 (b) CM120

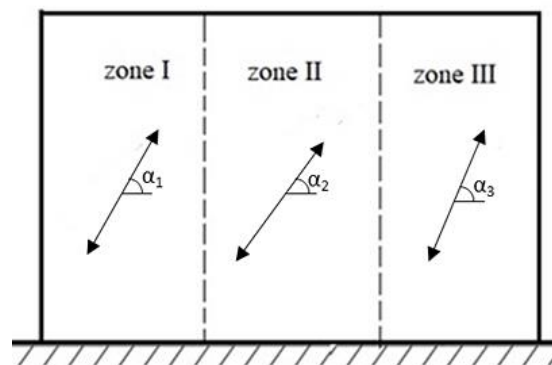


Figure 17. Three Zones of infill plates

Figure 18 illustrates the hysteretic curves of CS120 and CM120, which indicated that CS120 had wider loops and less pinching effect compared to CM120. However, the ultimate load of CM120 was 7.5% higher than that of CS120 as presented in Table 5.

Table 5. FE results of CS120 and CM120

Model	Corrugation Angle	Ultimate Load (kN)	Energy Dissipation Capacity (kN.m)	Toughness (kN.m)
CS120	120	524	1742.3	47.1
CM120	120	563	1767.6	49.9

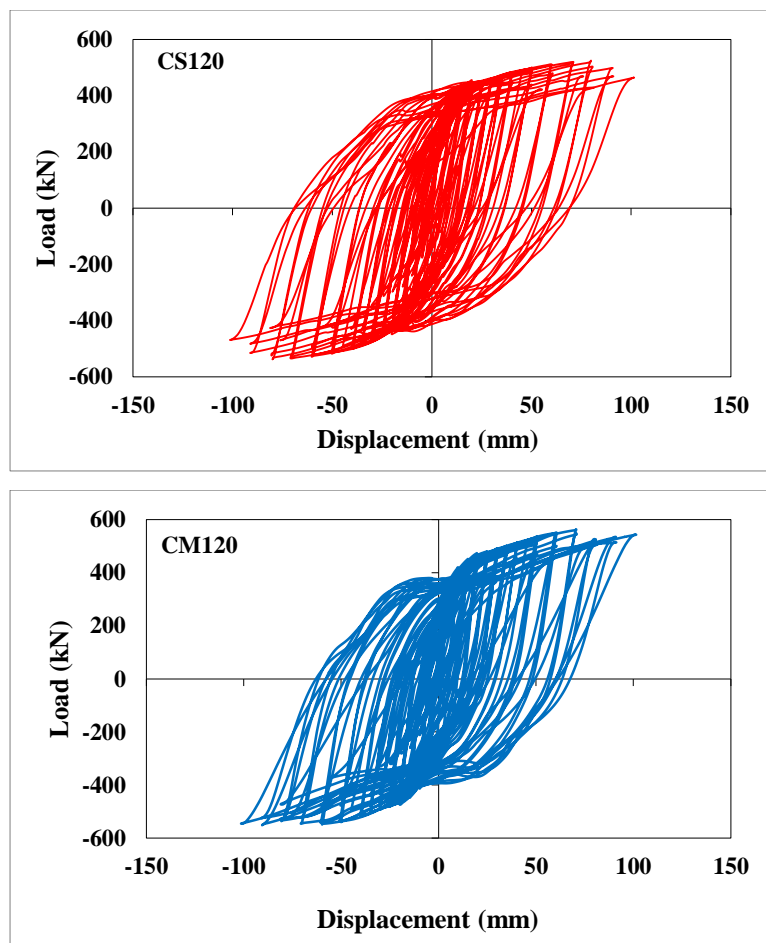


Figure 18. The hysteretic curves of CS120 and CM120

Figure 19 compares the ultimate loads of C120, CS120 and CM120 (V_{u-C}) with V_{u-FI} . The ultimate loads of CS120 and CM120 were 12% and 5% lower than V_{u-FI} , respectively. In addition, the results show that the ultimate loads of CS120 and CM120 were 3.5% and 11.8% higher than that of C120.

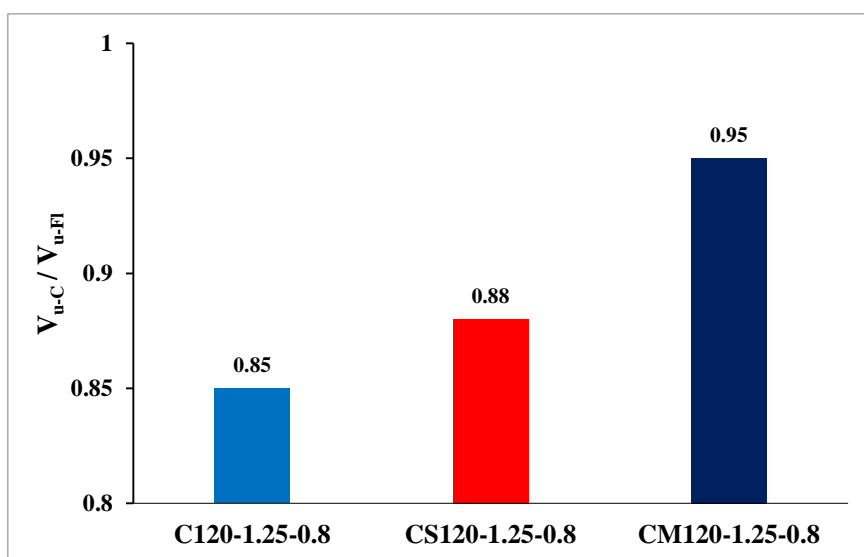


Figure 19. Comparison of the ultimate loads of C120, CS120 and CM120 with the ultimate load of FI

Figure 20 indicates the ratios of the energy dissipation capacities of C120, CS120 and CM120 to the energy capacity of the model with flat infill plate (DE_C / DE_{FI}). The results show that the energy dissipation capacities of CS120 and CM120 were 1.37% and 1.30 times greater than that of FI. Beside, CS120 and CM120 achieved considerably higher energy dissipation capacities compared to C120 as their energy dissipation capacities were 53.9% and 51.6% greater than that of C120, respectively.

The toughness of C120, CS120 and CM120 (T_C) were compared with T_{FI} in Figure 21. The comparison shows that CS120 and CM120 gained the toughness approximately 29% and 36% higher than that of the model with flat infill plate. Meanwhile, the toughness of C120 was 3.1% and 8.1% lower than those of CS120 and CM120, respectively.

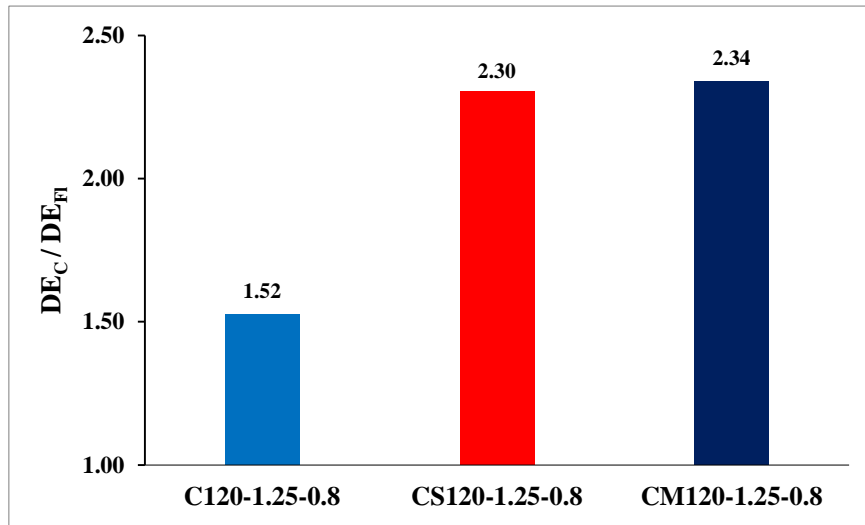


Figure 20. The ratios of the energy dissipation capacities of C120, CS120 and CM120 to the energy capacity of FI

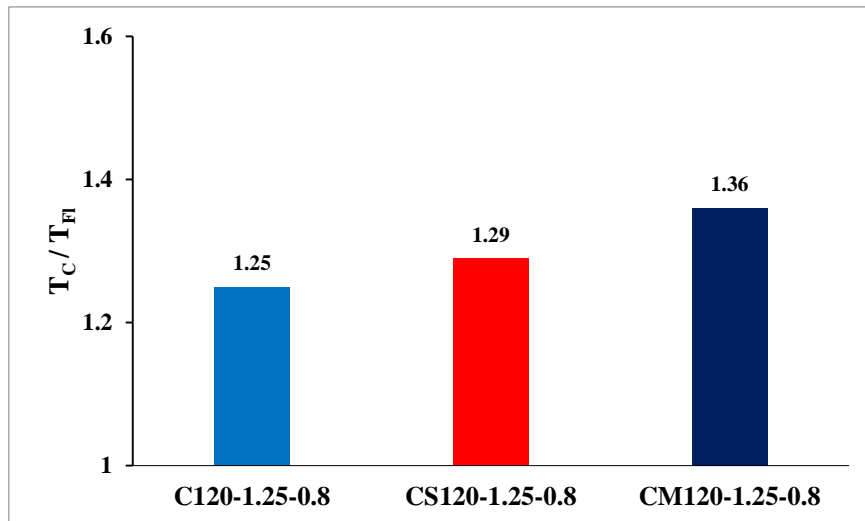


Figure 21. Comparison of the toughness of C120, CS120 and CM120 with the toughness of FI

The results reveal that CS120 and CM120 performed better than C120 as the ultimate loads, energy dissipation capacities and toughness were higher than those of C120. While, the amount of steel consumption for infill plates of CS120 and CM120 were 24.6% and 28.4% less than that of C120, respectively.

The reason of better performance of the proposed infill plates than flat plate through energy absorption and toughness could be attributed to the shear buckling of the plates (τ_{cr}) as presented in Equation 2 [9].

$$1/\tau_{cr} = 1/\tau_{cr,L} + 1/\tau_{cr,G}$$

$$\tau_{cr,L} = \frac{k\pi E}{12(1 - \nu^2)} \left(\frac{t}{a}\right)^2 \tag{2}$$

$$\tau_{cr,G} = 36\beta E [[(d/t)^2 + 2]/\eta]^{3/4} \left(\frac{t}{h}\right)^2 / 12(1 + \nu^2)$$

Where, E and ν are the elastic modulus, Poisson ratio, respectively. β and k are factors associated with the boundary condition of the infill plate. η is defined as $(a+b)/(a+c)$. a, b, c and d are the width of flat panel, the width of inclined panel, the projected width of inclined panel and corrugation depth, respectively. h is infill panel height.

Based on Equation 2, the infill of CM120 and CS120 gained higher τ_{cr} compared to FI, since the flat panel width (a) is shorter than that of FI. Thus, CM120 and CS120 (similar to CSSWs) can reach to greater displacement than FI, which could lead to higher energy dissipation capacity and toughness. In addition, due to superior shear strength of the

flat plate compared to the corrugated plate, CS120 and CM120 gained higher ultimate loads than that of C120. It's obvious that the proportion of flat plate can affect the ultimate load of the models. Therefore, the ultimate load of CM120 is greater than that of CS120, as its infill panel specified larger area of flat plate. However, the corrugated plate exhibited better performance in damping the lateral load. Hence, the energy dissipation capacity of CS120 was higher than that of CM120, because the proportion of the corrugated plate used in the infill panel of CS120 was greater. The damping effect of corrugated plate can be observed in the hysteretic behavior of CS120; in which the hysteresis loops CS120 showed minor pinching effect.

6. Conclusions

This study proposed new infill plate designs to improve the cyclic behavior of CSSWs as well as reducing the amount of steel used for infill panel. In this study, combinations of flat and corrugated plates were suggested based on a numerical investigation on the CSSW models with a variation of corrugation angle ranged from 30 to 120. According to the FE results, following conclusions were drawn:

- Based on the numerical investigation on the CSSW models with different corrugation angles, it was concluded that increasing corrugation angle from 30° to 120° improved the energy dissipation capacity and toughness up to 15% and 24.6%, respectively. In addition, C120 and C30 gained highest ultimate loads among the CSSW models.
- The proposed infill plate designs earned satisfactory results as the ultimate loads, energy dissipation capacities and toughness of CS120 and CM120 were up to 11.8%, 53.9% and 8.8% higher than those of C120, respectively. Meanwhile, the infill panels of CS120 and CM120 used 24.6% and 28.4% less steel material compared to that of C120, respectively.
- And it is concluded that using corrugated plate at the middle of the infill panel is a better option as the ultimate load and toughness of CM120 was greater 7.4% and 5.9% than those of CS120, respectively. While, its energy dissipation capacity was negligibly lower than that of CS120. Furthermore, infill panel of CM120 used 13.4% lower steel material compared to that of CS120.

7. Declarations

7.1. Author Contributions

Conceptualization, Methodology, Investigation Data Collection, Writing, Original Draft, Visualization and Validation, A.J.; Writing - Review & Editing M.A.; Review and Supervision, S.A.O.; Review and Supervision M.Y.M.Y.; All authors have read and agreed to the published version of the manuscript.

7.2. Data Availability Statement

The data presented in this study are available on request from the corresponding author.

7.3. Funding

The authors received no financial support for the research, authorship, and/or publication of this article.

7.4. Acknowledgements

I would like to thank Mohadeseh Rahmani Nia for her direction, sound guidance and kind assistance throughout this research.

7.5. Conflicts of Interest

The authors declare no conflict of interest.

8. References

- [1] Yu, Jin-Guang, Li-Ming Liu, Bo Li, Ji-Ping Hao, Xi Gao, and Xiao-Tian Feng. "Comparative Study of Steel Plate Shear Walls with Different Types of Unbonded Stiffeners." *Journal of Constructional Steel Research* 159 (August 2019): 384–396. doi:10.1016/j.jcsr.2019.05.007.
- [2] Wang, Meng, Xiaokang Zhang, Lu Yang, and Weiguo Yang. "Cyclic Performance for Low-Yield Point Steel Plate Shear Walls with Diagonal T-Shaped-Stiffener." *Journal of Constructional Steel Research* 171 (August 2020): 106163. doi:10.1016/j.jcsr.2020.106163.
- [3] Haddad, Omid, N. H. Ramli Sulong, and Z. Ibrahim, "Cyclic performance of stiffened steel plate shear walls with various configurations of stiffeners." *Journal of Vibroengineering* 20 (February 2018): 459–476. doi.org/10.21595/jve.2017.18472

- [4] Bahrebar, Milad, James B.P. Lim, George Charles Clifton, Tadeh Zirakian, Amir Shahmohammadi, and Mohammad Hajsadeghi. "Perforated Steel Plate Shear Walls with Curved Corrugated Webs Under Cyclic Loading." *Structures* 24 (April 2020): 600–609. doi:10.1016/j.istruc.2020.01.047.
- [5] Hosseinpour, Emad, Shahrizan Baharom, and Yasser Yadollahi. "Evaluation of Steel Shear Walls Behavior with Sinusoidal and Trapezoidal Corrugated Plates." *Advances in Civil Engineering* 2015 (2015): 1–11. doi:10.1155/2015/715163.
- [6] Shon, Su-Deok, Mi-Na Yoo, Seung-Jae Lee, and Joo-Won Kang. "A Comparative Study on Shear Buckling and Interactive Buckling Characteristics of Trapezoidal and Sinusoidal Corrugated Steel Plate." *Journal of the Architectural Institute of Korea Structure & Construction* 31, no. 4 (April 30, 2015): 39–46. doi:10.5659/jaik_sc.2015.31.4.39.
- [7] Berman, Jeffrey W., and Michel Bruneau. "Experimental Investigation of Light-Gauge Steel Plate Shear Walls." *Journal of Structural Engineering* 131, no. 2 (February 2005): 259–267. doi:10.1061/(asce)0733-9445(2005)131:2(259).
- [8] Shon, Sudeok, Mina Yoo, and Seungjae Lee. "An Experimental Study on the Shear Hysteresis and Energy Dissipation of the Steel Frame with a Trapezoidal-Corrugated Steel Plate." *Materials* 10, no. 3 (March 6, 2017): 261. doi:10.3390/ma10030261.
- [9] Emami Fereshteh, Massood Mofid, and Abolhassan Vafai. "Experimental Study on Cyclic Behavior of Trapezoidally Corrugated Steel Shear Walls." *Engineering Structures* 48 (March 2013): 750–762. doi:10.1016/j.engstruct.2012.11.028.
- [10] Farzampour, Alireza, Iman Mansouri, and Jong Wan Hu. "Seismic Behavior Investigation of the Corrugated Steel Shear Walls Considering Variations of Corrugation Geometrical Characteristics." *International Journal of Steel Structures* 18 (July 2018): 1297–1305. doi:10.1007/s13296-018-0121-z.
- [11] Bahrebar, Milad, Mohammad Zaman Kabir, Tadeh Zirakian, Mohammad Hajsadeghi, and James B.P. Lim. "Structural Performance Assessment of Trapezoidally-Corrugated and Centrally-Perforated Steel Plate Shear Walls." *Journal of Constructional Steel Research* 122 (July 2016): 584–594. doi:10.1016/j.jcsr.2016.03.030.
- [12] Bahrebar, Milad, Tadeh Zirakian, and Mohammad Hajsadeghi. "Nonlinear Buckling Analysis of Steel Plate Shear Walls with Trapezoidally-Corrugated and Perforated Infill Plates." In *Proceedings of the Annual Stability Conference, Structural Stability Research Council* (2015).
- [13] Hosseinzadeh, Leila, Fereshteh Emami, and Masood Mofid. "Experimental Investigation on the Behavior of Corrugated Steel Shear Wall Subjected to the Different Angle of Trapezoidal Plate." *The Structural Design of Tall and Special Buildings* 26, no. 17 (July 2017): e1390. doi:10.1002/tal.1390.
- [14] Fadhil, Hayder, Amer Ibrahim, and Mohammed Mahmood. "Effect of Corrugation Angle and Direction on the Performance of Corrugated Steel Plate Shear Walls." *Civil Engineering Journal* 4 (November 2018): 2667. doi:10.28991/cej-03091190.
- [15] Berman, Jeffrey, and Michel Bruneau. "Plastic analysis and design of steel plate shear walls." *Journal of Structural Engineering* 129, no. 11 (2003): 1448-1456. doi:10.1061/(ASCE)0733-9445(2003)129:11(1448)
- [16] Lv, Yang, Ling Li, Di Wu, Bo Zhong, Yu Chen, and Nawawi Chouw. "Experimental Investigation of Steel Plate Shear Walls Under Shear-Compression Interaction." *Shock and Vibration* 2019 (March 18, 2019): 1–11. doi:10.1155/2019/8202780.